Fusion, space and solar plasmas as complex systems

R O Dendy[1,2]**, S C Chapman**[2] **and M Paczuski**[3]

[1] Euratom/UKAEA Fusion Association, Culham Science Centre, Abingdon, Oxfordshire, OX14 3DB, UK
[2] Centre for Fusion, Space and Astrophysics, Department of Physics, Warwick University, Coventry, CV4 7AL, UK
[3] Department of Physics and Astronomy, University of Calgary, 2500 University Drive NW, Calgary, Alberta T2N 1N4, Canada

Abstract

Complex systems science seeks to identify simple universal models that capture the key physics of extended macroscopic systems, whose behaviour is governed by multiple nonlinear coupled processes that operate across a wide range of spatiotemporal scales. In such systems, it is often the case that energy release occurs intermittently, in bursty events, and the phenomenology can exhibit scaling, that is a significant degree of self-similarity. Within plasma physics, such systems include Earth's magnetosphere, the solar corona and toroidal magnetic confinement experiments. Guided by broad understanding of the dominant plasma processes—for example, turbulent transport in tokamaks or reconnection in some space and solar contexts—one may construct minimalist complex systems models that yield relevant global behaviour. Examples considered here include the sandpile approach to tokamaks and the magnetosphere and a multiple loops model for the solar coronal magnetic carpet. Such models can address questions that are inaccessible to analytical treatment and are too demanding for contemporary computational resources; thus they potentially yield new insights, but risk being simplistic. Central to the utility of these models is their capacity to replicate distinctive aspects of observed global phenomenology, often strongly nonlinear, or of event statistics, for which no explanation can be obtained from first principles considerations such as the underlying equations. For example, a sandpile model, which embodies critical-gradient-triggered avalanching transport associated with nearest-neighbour mode coupling and simple boundary conditions (and little else), can be used to generate some of the distinctive observed elements of tokamak confinement phenomenology such as ELMing and edge pedestals. The same sandpile model can also generate distributions of energy-release events whose distinctive statistics resemble those observed in the auroral zone. Similarly, a multiple loops model, which embodies random footpoint motion combined with reconnection of intersecting loops (and little else), can generate global magnetic field structure resembling

the solar coronal magnetic carpet, with power law distributions for energy-release events also similar to those observed in the solar corona. These reduced models thus focus on identifying the key physical ingredients that are necessary and sufficient to generate the observed phenomenology.

1. Introduction

Finding simple physical systems whose global behaviour resembles that of large-scale plasmas is important, for at least two reasons. First, it assists the identification of the dominant physical processes that govern the observed phenomenology. This is otherwise difficult, given the many interacting plasma physics mechanisms, operating on diverse lengthscales and timescales and in nonlinear regimes, that combine together to produce the effects observed. Second, it assists the identification of a small set of key control parameters—perhaps representing the combined effects of many experimental variables—whose values determine system behaviour. A simple model that captures the key physics can thus provide a means to understand and control the integrated system behaviour. This is particularly helpful in situations that are analytically intractable, for example because of strongly nonlinear characteristics or are inaccessible to direct numerical simulation because of computational resource limitations.

Considerations of this kind are by no means unique to plasma physics. It is widely recognized that for nonlinear dissipative systems in general, knowledge of the governing equations is seldom sufficient to predict or interpret the global phenomenology that is observed. Collective effects acting in systems having a large number of degrees of freedom, acting over many lengthscales and timescales, give rise to self-organized emergent phenomenology that cannot be predicted from the equations describing the elements of the system. Computational approaches can provide a valuable guide to emergent behaviour but are constrained by resource limitations that are not necessarily merely technological, to be overcome in a few years' time. The number of degrees of freedom is typically so large, and the spread of lengthscales and timescales so extensive, as to prohibit the construction of a set of direct numerical simulations sufficiently comprehensive to capture all aspects of the emergent behaviour. The field of complex systems science [1–3] has arisen to meet this challenge during the past two decades. Complex systems science offers two types of approach that are particularly helpful in plasma physics. First, there is now an array of statistical physics techniques that are specially adapted to capturing and quantifying the nonlinear features of macroscopic system behaviour. Unfortunately there is not enough space to describe these in the present paper (a review [4] is in preparation), and we refer the interested reader elsewhere for applications to a variety of plasmas including astrophysical accretion discs [5, 6], the solar corona [7], the solar wind and terrestrial ionosphere [8, 9], edge fluctuations in the MAST tokamak [10] and ELM statistics in the JET tokamak [11]. The second avenue offered by complex systems science comprises simple physically motivated conceptual models of the kind adumbrated in the preceding paragraph. In plasma physics, the most familiar complex systems paradigm is the sandpile [12–19], some of whose successes we explore in the present paper, before moving on to a novel approach to the multiple interactions of multiscale magnetic loops in the solar corona.

2. Complex systems models for global tokamak phenomenology

There is now substantial experimental evidence that simple diffusive and Gaussian paradigms for the transport arising from turbulence in tokamak plasmas are insufficient to describe
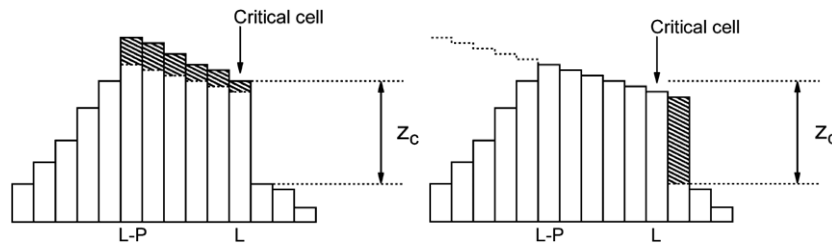
Figure 1. Section of sandpile prior to flattening (left) and after flattening (right), for the case $L_f = 6$. The gradient at the critical cell initially exceeds z_c, so that sand from this cell and its five nearest leftward neighbours is transported downhill to its nearest rightward neighbouring cell. From [36], for which see further discussion of boundary conditions.

all the confinement phenomenology observed. Early classic measurements of avalanching transport include [20, 21]; analysis of edge plasma turbulence measurements, see for example [10, 19,22–27], yields non-Gaussian probability distribution functions that are long-tailed and may be inverse power law, pointing towards intermittency and perhaps self-organized criticality; and self-organized bursty transport is seen in a wide range of numerical simulations [28–33]. In parallel to these developments, there remains the outstanding physics question arising from observations of tokamak plasma confinement: namely, *why* the distinctive characteristics—enhanced confinement regimes, edge pedestals, ELMs and so on—arise *at all*. For example, are these phenomena sufficiently generic that their existence could in principle have been predicted by analogy with other physical systems? Both *a priori* and observational plasma physics considerations thus motivate exploration of the sandpile paradigm for rapid nonlocal nondiffusive transport events arising from critical gradient-triggered nearest-neighbour interactions.

Here we consider tokamak applications of the simple one-dimensional sandpile model of [16] (hereafter CDH), which incorporates other established models [12, 15] as limiting cases. The centrally fuelled (at cell $n = 1$) CDH model's distinctive algorithmic feature relates to the local redistribution of sand at a cell (say at $n = k$) when the critical gradient z_c is exceeded there. The sandpile is flattened behind the unstable cell over a 'fluidization length' L_f, embracing the cells $n = k - (L_f - 1), k - (L_f - 2), \ldots, k$; and this sand is conservatively relocated to the cell at $n = k + 1$; see figure 1. As in all sandpile models, the system is then iterated to stability, generating an avalanche (of whatever size), before it is fuelled again. Physically, the lengthscale L_f, which governs rapid redistribution, may be considered to be a proxy for turbulent vortex size, for example. The limit $L_f = 1$ is the fixed point corresponding to the centrally fuelled algorithm of [12] in one dimension. In the limit $L_f = N$ (where N is the number of cells in the sandpile), the sandpile is flattened everywhere behind an unstable cell as in [15, 34]. The CDH sandpile has been explored [16] for all regimes $1 < L_f < N$ for both constant and fluctuating critical gradient z_c. In the more realistic case with random fluctuations in z_c, the system is robust in that the behaviour is essentially insensitive to the fluctuation level and spectral properties [16, 34]. The sole control parameter is the normalized redistribution scalelength L_f/N, which gives rise to different regimes of avalanche statistics and dynamics.

It is shown in [18, 35, 36] that the CDH sandpile model displays phenomenology similar to the following aspects of tokamak confinement phenomenology: edge pedestals and enhanced confinement [18], see figure 2 (left); ELMing [18], see figure 2 (right); the dependence of ELM frequency on stored energy [18], see figure 3; internal transport barriers [35]; and off-axis
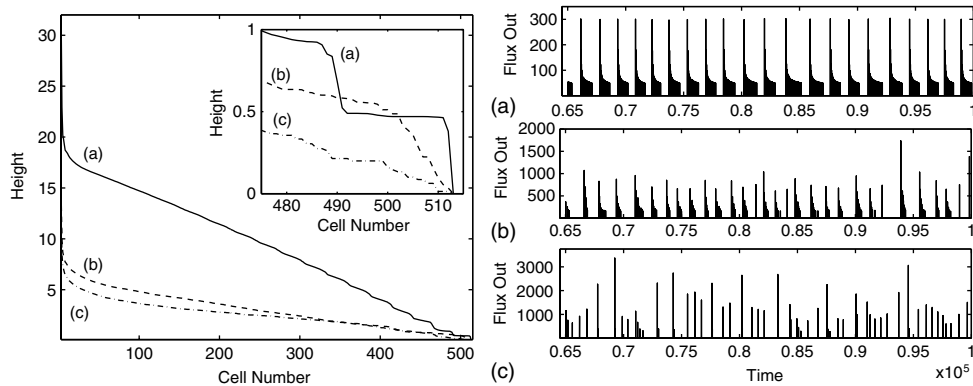
Figure 2. Enhanced confinement, edge pedestals and pulsed mass loss events in a sandpile, see [18]. (left): time averaged height profiles of the 512 cell sandpile for $L_f =$ (*a*) 50, (*b*) 150, (*c*) 250. Inset: edge structure. (right): time series of external avalanches (MLEs) for the 512 cell sandpile for $L_f =$ (*a*) 50, (*b*) 150, (*c*) 250; these plots show magnitude of flux leaving the sandpile, versus time.

ECRH temperature profiles [36], which are examined further in section 3. The existence of enhanced confinement and edge pedestals for this sandpile is complemented by the pulse-like time series for its external avalanches ('mass loss events' (MLEs), see figure 2 (right)), whose role mimics that of ELMs in tokamak plasmas. Not only does the character of the MLEs correlate with the confinement properties of the sandpile, there are also quantitative correlations. For example, figure 3 shows the scaling of the frequency of the MLEs with stored energy in the sandpile, which is similar in form to that obtained for the scaling of ELM frequency with stored energy in JET for certain plasmas, see figure 6 of [37]. From a rigorous complex systems perspective, figure 3 is also important in that it confirms that the sandpile phenomenology is robustly scale-invariant with respect to the number N of cells chosen in the implementation of the sandpile model.

A related line of research aims to identify the minimal requirements for statistical processes that can generate nondiffusive avalanching transport and can reproduce, for example, the non-Gaussian features of density fluctuation and flux fluctuation measurements in tokamaks. It has been shown [19,27] that statistical clustering of transport events, described for example in terms of contemporary models for population dynamics [19] or of Lévy processes [27], is sufficient to generate some of the observed phenomenology. For example, figure 1 of [19] displays the time series of time-integrated local height fluctuations from a simple sandpile model that can be characterized in these terms. The mathematical derivation of this trace from the local sandpile height is equivalent to that of the random walk constructed from local edge density measurements in the DIII-D tokamak in [26]. Not only is there visual similarity between the output of the sandpile model and the tokamak measurements of figure 2(*a*) of [26], but there are also quantitative points of contact that emerge when nonlinear time series analysis is applied [19] to compute figures-of-merit such as the Hurst exponents, which are also explored in the context of astrophysical [5] and MAST tokamak [10] plasmas.

The emergence, from a very simple system [16], of counterparts to several aspects of tokamak confinement phenomenology [18, 35, 36], is interesting. Insofar as the resemblance is close, there is more to be learned. A minimalist interpretation starts from the premise that this sandpile algorithm provides a simple one-parameter model for studying generic nonlocal transport, conditioned by a critical gradient, in a macroscopic confinement system. Changing
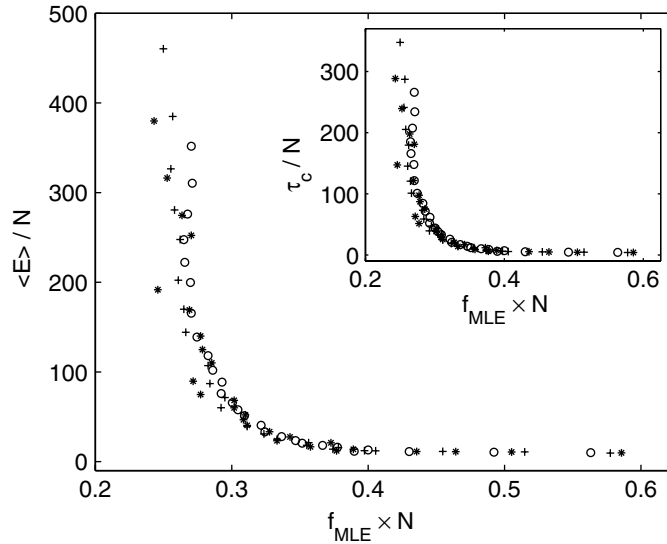
Figure 3. Averaged stored energy versus frequency of MLEs for the sandpile with number of cells $N = 512, 4096$ and 8192, see [18]. Normalization with respect to N shows robust scale invariance of this phenomenology. Inset: plot of confinement time versus MLE frequency shares features with measured correlation [37] of energy confinement with ELM frequency in some JET plasmas.

the value of the single control parameter L_f then corresponds to altering the spatial range over which the transport process operates; different values of L_f would reflect different properties of the plasma turbulence underlying the transport. It then follows from the above results that this small set of mathematical ingredients may be the minimum required to generate the aspects of tokamak-like confinement phenomenology that we have found. This is significant, but one can also consider a more far-reaching interpretation. This maximalist interpretation attaches greater weight to the observations [20–33] of avalanching transport in tokamaks and in largescale numerical simulations thereof, and therefore regards the avalanching transport that is built into sandpile algorithms as an additional point of contact with the physics of magnetically confined plasmas. One would then infer from the results reviewed here that tokamak observations of avalanching transport are deeply linked to the existence of enhanced confinement and ELMs. Furthermore the existence of the single control parameter L_f, governing the confinement phenomenology and arising from the rapid transport, would then hold out the prospect of a synthesis of the many experimental parameters into a very small number of underlying control parameters. We note also that large L_f corresponding to low confinement (trace (c) of figure 2 (left)), is known [16, 18] to correspond to robust scale-free systems dynamics; whereas small L_f, corresponding to high confinement (trace (a) of figure 2 (left)), does not give rise to self-similar dynamics. A testable conjecture concerning the nature of the high and low confinement regimes in tokamaks thus arises, if we choose to proceed by analogy with the sandpile. The H-mode would correspond to low-dimensional behaviour, with the dynamics of the core only loosely coupled to quasi-oscillatory edge dynamics; while the L-mode would correspond to high-dimensional behaviour, with coupling extending across the system. Having now explored broad confinement physics issues, in the next section we consider the sandpile modelling of a single highly technical aspect of tokamak behaviour.
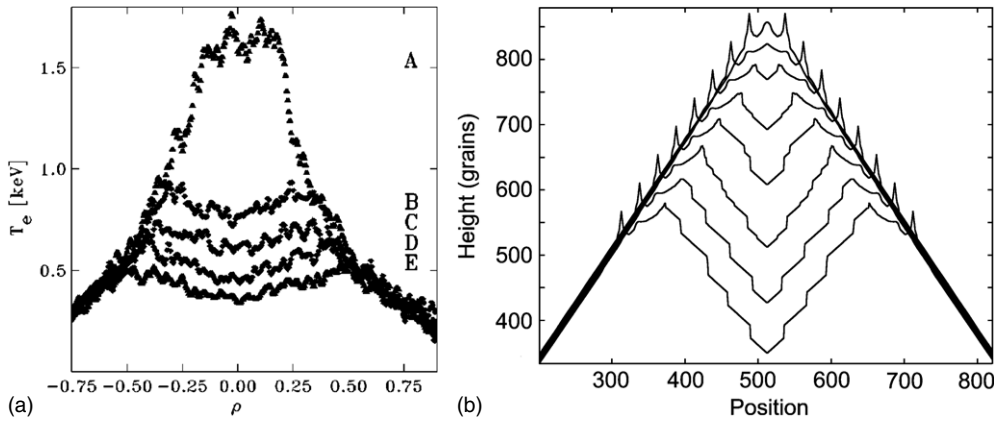
Figure 4. Similarity between global profiles in off-axis fuelled plasma and sandpile. (Left): examples of electron temperature profiles measured from a series of RTP tokamak plasmas undergoing ECH at different off-axis locations, reproduced from [41]. (Right): examples of average height profiles for a series of runs of the sandpile model fuelled at different off-axis locations, reproduced from [36].

3. Complex systems modelling of off-axis electron cyclotron heating in tokamaks

Electron cyclotron heating (ECH) provides a means for delivering energy to a region of a toroidal fusion plasma that is highly localized in the radial spatial coordinate. This localization follows from the nature of the cyclotron resonant condition between the incident waves and the electrons. Rapid transport of heat along magnetic field lines ensures that, initially, ECH energy is swiftly and evenly spread over the family of nested toroidal magnetic surfaces on which it was first deposited, whose radial extent is relatively narrow. On longer timescales, radial transport of this energy across the plasma is governed by the physics of electron energy transport perpendicular to the applied magnetic field, which includes turbulent processes, and by the radial temperature gradient, to which energy deposited through ECH both responds and contributes. Observations of the response of toroidal plasmas to ECH thus provide a probe of the underlying physics of transport and confinement, particularly when advantage is taken of the capability to localize ECH spatially and temporally. The classic off-axis ECH experiments (having non-central energy deposition) reported on the DIII-D [38, 39] and Rijnhuizen Tokamak Project (RTP) [40,41] experiments are particularly interesting in this respect. As noted by the experimenters, it is clear that their results contain information on the balance between diffusive and nondiffusive (for example, avalanching) transport processes. One way of extracting some of this information is to investigate how far the sandpile paradigm can capture key aspects of the plasma behaviour which is observed. This applies particularly to features of the observed plasma behaviour that are strongly nonlinear, and therefore difficult to capture using the conventional analytical techniques of plasma physics. This question has been examined for both DIII-D and RTP in [36]; here we focus on results relating to off-axis ECH in the RTP tokamak.

The left side of figure 4 (figure 8 of [41]) shows electron temperature profiles obtained in the RTP tokamak for different off-axis locations of energy deposition. The extremely high resolution of the Thomson scattering techniques used in RTP yields two major benefits. First, the number of data points in the spatial profiles is very high. Second, the location of the peak ECH energy deposition point with respect to the measured sequence of radial transport
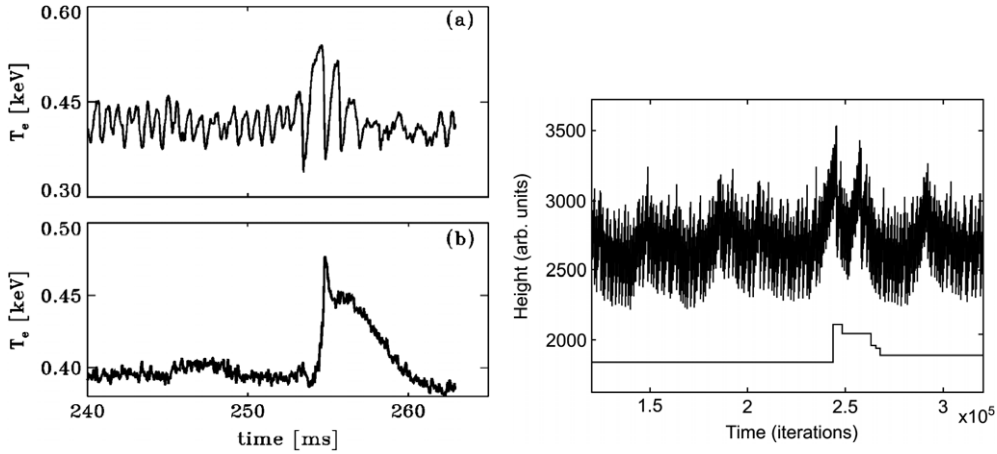
Figure 5. Similarity between time evolution of correlated local fluctuations in off-axis fuelled plasma and sandpile, showing minor crashes and one major crash. (Left): time evolution of electron temperature in an RTP tokamak plasma, measured at (*a*) the off-axis ECH position and (*b*) the centre, reproduced from [40]. (Right): time evolution of sandpile height, measured at (upper) the off-axis fuelling position and (lower) the centre, reproduced from [36]. The horizontal (time) axis is measured in number of sand grains added; control parameter $L_f = 200$.

barriers is well determined. Figure 4 (left) shows that as the off-axis deposition location is moved outwards, correspondingly broader hollow electron temperature profiles result. In parallel, the peak central temperature falls, while the outboard gradient is almost invariant. The CDH sandpile model enables us to test [36] whether these observations are consistent with the idea that the plasma transport incorporates an avalanching component conditioned by a critical gradient. Figure 4 (right) shows sets of height profiles for a CDH sandpile with 512 cells, averaged over 10^9 sand grains, for different off-axis locations of sand deposition, with $L_f = 50$ in all cases. For comparison with the tokamak profiles of figure 4 (left), which extend across the plasma from the inner to the outer boundaries, figure 4 (right) shows sandpile profiles obtained by mirroring the final data about the pile centre. The centre of the sandpile is labelled cell number $n = 1$, and separate profiles are obtained for off-axis fuelling locations at cells $25, 50, \ldots, 200$. There are four points of contact between the form of the sandpile height profiles on the right of figure 4 and the RTP electron temperature profiles on the left of figure 4. First, there are hollow profiles whose central height falls as the fuelling location is moved further off-axis. Second, for fuelling locations that are not far off-axis, the inboard portion of the profile (between the fuelling location and the centre) is approximately flat. Third, the outboard profile (between the fuelling location and the outer edge) is independent of fuelling location. Fourth, there are 'ears' near the deposition point.

Now let us consider figure 6 of [40], shown here on the left of figure 5. This shows two points of particular interest. First, in the run-up to the major crash in central electron temperature in RTP, which occurs at $t \approx 253$ ms, the amplitude of temperature fluctuations is greater at the ECH deposition point than at the centre. Second, the major crash has a more sharply defined leading edge measured at the centre; thereafter it relaxes almost monotonically, whereas the temperature at the deposition point oscillates several times during this interval. Figure 5 (right) shows that similar behaviour occurs naturally in our sandpile model. The upper trace shows the time evolution of the height of the sandpile at its off-axis fuelling point ($n = 100$), while the lower trace shows the simultaneous time evolution of the height of the

sandpile at its central cell ($n = 1$ here). Here the degree of similarity between plasma and sandpile extends to the shape of these strongly nonlinear signals. Common features include the double-pulse structure of the major crash at the fuelling point and the up–down–across–down structure of the major crash at the centre, which occurs slightly later than the crash at the fuelling point in both cases. Together, figures 4 and 5 suggest that critical-gradient-conditioned avalanching transport may play a significant role in generating the observed plasma phenomenology.

4. Complex systems modelling of Earth's magnetosphere

Earth's magnetosphere fundamentally resembles a tokamak, in that it is a macroscopic magnetic confinement system for plasma set up by the interaction between a flow—the solar wind, instead of a toroidal current—and a magnetic field anchored in dense electrically conducting matter—the Earth's core, instead of copper or superconducting coils. Both tokamaks and the Earth's magnetosphere are driven-dissipative plasma systems that combine energy injection, storage and distinct release events; and both exhibit structure and display plasma phenomenology on a very broad range of lengthscales and timescales. Here too, in the search for unifying paradigms, complex systems science appears to offer guidance; for a recent accessible review, see for example [42]. In the present paper we focus on applications of the CDH sandpile model introduced in the preceding sections. Motivation for the sandpile approach to the magnetosphere arises both on these *a priori* grounds and observationally, through analysis of the statistics of energy release events, for example. Terrestrial magnetometer measurements of geomagnetic indices, which reflect energy deposition in the auroral zone arising from plasma transport of energy released in distant reconnection events in the magnetotail, can yield scale-free power law distributions [43, 44] resembling those of avalanching processes in sandpiles, as was noted in [45, 46] reviewed further in [47, 48]. These statistics appear to be intrinsic [49] to the internal plasma physics of the magnetosphere, as distinct from being conditioned by the ultimate driver, the solar wind.

The sandpile model of [46] yields both internal avalanches (involving transport of sand within the system but no mass loss) whose distribution is scale-free and external avalanches (involving transport of sand right across the system, resulting in some loss of sand) whose distribution has a well-defined mean and hence an intrinsic scale. At the simplest level, then, this model could in principle encompass both intermittent local magnetospheric energy release events, arising for example from bursty bulk flows and pseudobreakups, as well as global energy release events, such as substorms. Furthermore the model is known to be robust [48, 50] against substantial temporal fluctuations in the magnitude of the fuelling and against different rates of fuelling. For example, figure 6 (from [48]) plots the distribution of avalanche energy against the number of events for two types of central fuelling: slow (diamonds) and fast (circles). This is important for space and astrophysical applications where the driver may be highly variable, for example the solar wind, and differs from the classical self-organized criticality [1] picture of slowly driven dynamics. The rollover at small energies in figure 6 reflects the minimum size of discrete energy packets with which the systems are fuelled; both distributions display a robust power law with slope-1 at higher energy; and the distinct distribution of systemwide avalanches with a well-defined mean is visible at the highest energies.

The similarity between figure 6 and the observed distribution of certain magnetospheric energy release events, reproduced here as figure 7, was noted by Lui *et al* in [51]. Global snapshot images of ultraviolet emission across the entire auroral oval (see, for example, figure 3 of [42]) were routinely obtained by the POLAR UVI instrument looking down on Earth. Analysis [51] of 9033 images taken during January 1997 gives rise to the magnitude–frequency
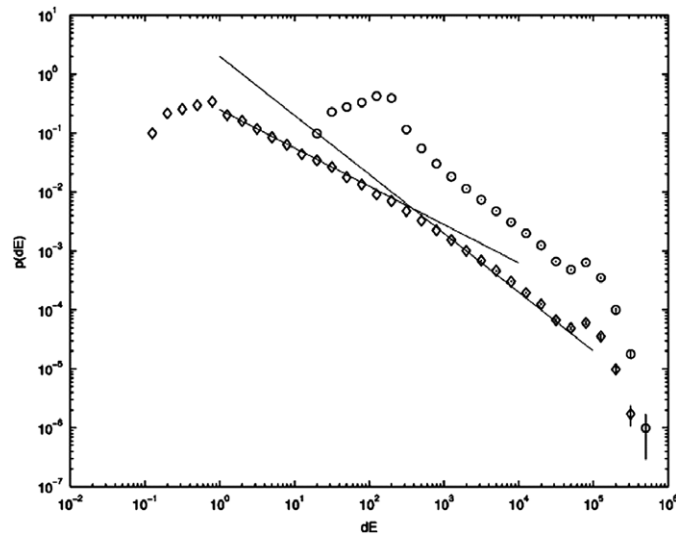
Figure 6. Logarithmic plot of the measured distribution $p(dE)$ of avalanche energy dE in a 5000 cell CDH sandpile with $L_f = N$, for two central fuelling rates: slow ($\diamondsuit$) and ten times faster ($\bigcirc$). Rollover at left reflects finite size of discrete fuelling events; power law slope is -1 above $dE = 10^3$; systemwide avalanches are visible at right, peaking near $dE = 10^5$. From [48].
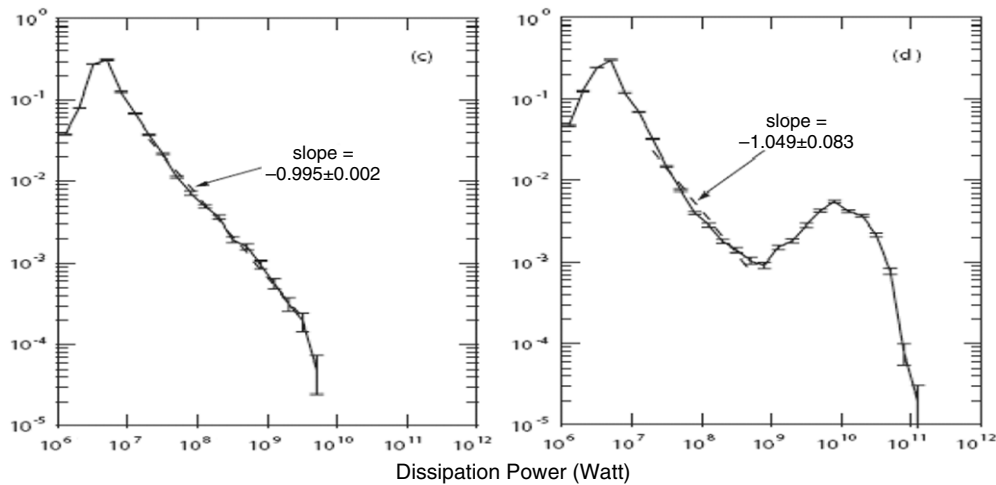
Figure 7. Observed logarithmic frequency–magnitude plots of UV emission from Earth's auroral oval obtained by the POLAR UVI instrument. (Left): quiet. (Right): concurrent substorm activity. Comparison with figure 6 suggests that the sandpile and magnetosphere share global phenomenology, with substorms driving systemwide avalanches. From [51].

plots of figure 7. The data are split into two categories: active (figure 7 (right)), when there is concurrent substorm activity in the magnetotail, which gives rise to spatially extended UV emission spanning the auroral oval, and quiet (figure 7 (left)), when substorm activity is absent, and auroral UV emission consists of more localized blobs. There is a straightforward mapping between the salient features of figure 7 (right) and those of figure 6: the observed event distribution of UV emission from the auroral oval matches that from a sandpile that has
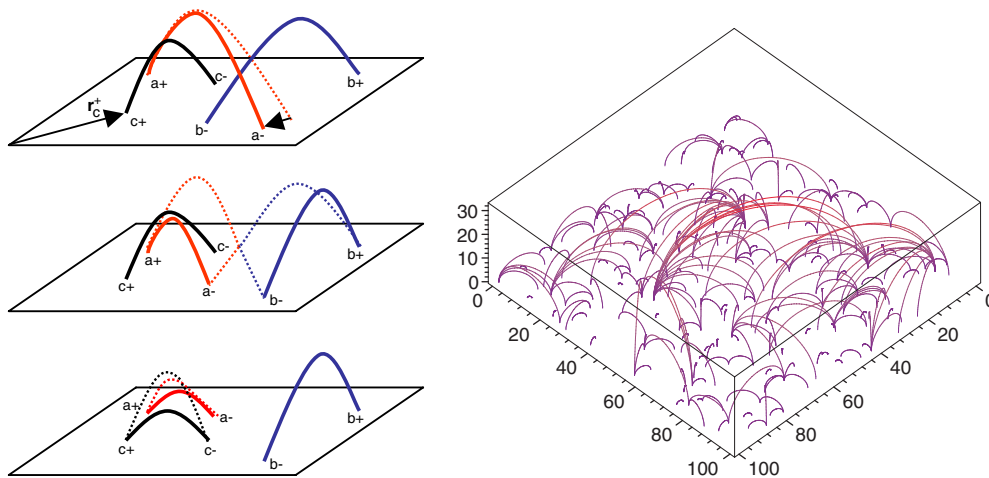
Figure 8. (Left): diagram showing the process of a reconnection event in the multiple loops model of [54]. In the top frame, loop a moves from its previous position (dashed line) and crosses loop b. Subsequently (middle frame) the loops exchange footpoints and move to their final relaxed configuration (bottom frame). (Right): snapshot of a configuration of multiple loops in steady state; see online [54] for a colour version.

blobby fuelling and displays both systemwide and internal avalanches. Identification of the systemwide avalanches with substorms, and of the internal avalanches with an ever-present process of auroral activity, is reinforced by figure 7 (left). Taken at times when substorms are absent, figure 7 (left) has no population of large events with well-defined mean, unlike figure 7 (right), but displays the same distribution of smaller scale events which are fitted by a power law. The fact that this slope is independent of the level of activity in the system suggests that it reflects continual underlying intermittent bursts associated with internal reconfiguration.

5. A global complex systems model for aspects of solar coronal plasma and magnetic fields

According to the physical picture proposed by Parker, magnetic loops are pushed out of the solar photosphere into the corona with an inhomogeneous flux pattern anchored to the photosphere. Turbulent plasma flow on the photospheric surface drives the anchored flux loops into complex, stressed configurations [52]. When local magnetic field gradients become sufficiently steep, plasma instability allows the coronal magnetic field to change its topology via reconnection, suddenly releasing energy [53]. A cascade of reconnecting flux loops may be a mechanism underlying solar flares, with the larger flares originating in regions of strong coronal fields.

A complex systems model applicable to solar coronal magnetic fields has been proposed [54] where multiple directed loops evolve in space and time. Unlike a sandpile model, this multiple-loops model aims to capture the essentially topological nature of reconnection events in the solar coronal plasma. In this multiple loops dynamic model [54], therefore, a pair of footpoints, having opposite polarity, anchors each directed loop to a two-dimensional surface, representing the photosphere. These multiple magnetic loops undertake randomly driven motion at their footpoints, and can interact. Nearby footpoints of the same polarity aggregate; furthermore when loops intersect they can reconnect (see figure 8 (left)) by exchanging footpoints, if this lowers the combined length of the pair.
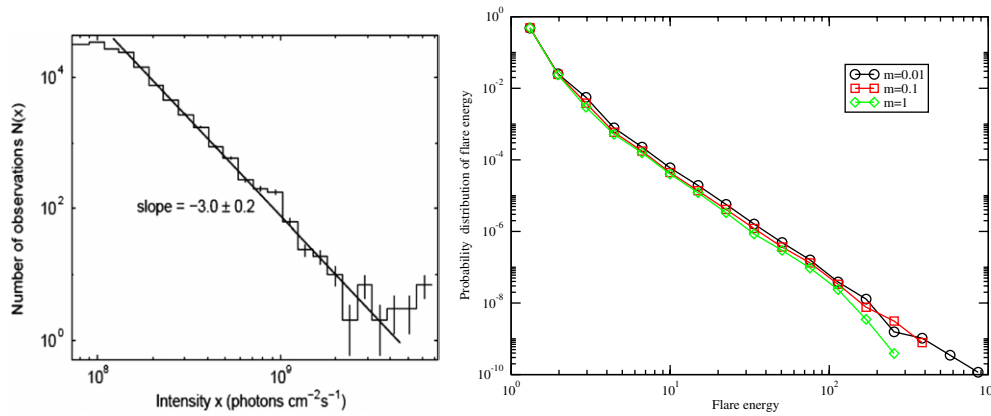
Figure 9. Similarity between distributions of magnitudes of energy release events observed for the solar corona and obtained from the multiple loops model: a power law with index -3 in both cases. (Left): logarithmic plot of number of observations $N(x)$ of detrended full-disc solar flux intensity x, measured at 15 s intervals by SOHO/SEM from January to June 1996, reproduced from [7]. (Right): logarithmic frequency–magnitude plot of energy release events occurring in the multiple loops model, reproduced from [54].

Depending on the local density of neighbouring loops, and their configuration, a single reconnection can lead to further loop interactions and thereby trigger a cascade of further reconnection. These cascades lower the overall length of loops in the system and are identified with the energy release events underlying solar flares. Loops are injected at small scales, so that, combined with random footpoint motion, an energetic and statistical steady state is achieved.

Numerical implementation [54] of this model gives rise to loop configurations (see figure 8 (right)) that are qualitatively similar, in the steady state, to the magnetic carpet deduced from observations of the photospheric field [55]. The term magnetic carpet refers to the structure of field lines embedded in the coronal plasma, in regions that are not dominated by major structures such as flares, prominences and active regions. The model yields a pattern of loops that dynamically forms a scale-free network, where the number of loops emerging from each footpoint is distributed as a power law; we note that this is a prediction, which could be tested by solar magnetic field observations in future. Furthermore a power law distribution of flare energies emerges from the model. Perhaps significantly, the power law index ≈ -3 obtained [54] from the model is the same as that measured [7] for full-disc EUV/XUV solar irradiance during a low activity period in 1996; see figure 9, which compares figure 4 of [54] with upper figure 2 of [7]. The model outcomes resonate with the observed statistics of peak flare x-ray flux distributions [56], of the energy released [57], and of the quiescent time intervals between solar flares [58]: these are all characterized by power law distributions, with power law indices that are independent of the phase of the solar cycle [59]. The distribution of energy released is particularly striking, exhibiting scale-free behaviour over more than eight decades in energy. It is well known [60] that these statistics indicate that the solar corona may be in a state of SOC, sharing some common features with other intermittent scale-free phenomena such as earthquakes, forest fires, biological evolution, traffic and turbulence [1–3,61].

This complex systems model [54] of the solar coronal magnetic field, consisting of multiple driven reconnecting magnetic loops, is designed to capture essential elements of the local physics governing such structures and their interactions. Importantly, it leads to a global description that involves many more loops, and extends over greater lengthscales and

timescales, than are accessible to traditional analytical and computational techniques based on the underlying equations. The striking—and unpredictable—outcome of the multiple loops reconnection model is the dynamical self-organization of the magnetic field embedded in the coronal plasma, which gives rise to a power law distribution of solar flare energies and which forms a scale-free network that qualitatively resembles the actual coronal magnetic field. This outcome is presumably not dependent on the specific details of the rules of the multiple loops model. From a complex systems perspective, the suggestion is that the solar coronal magnetic field behaves globally as it does because that is where it is led by the key physics elements, as captured in the much simpler multiple loops model.

6. Conclusions

Fortuitous coincidence is an unlikely explanation for the points of contact between complex systems paradigms and the observed phenomenology of fusion, space and solar plasmas that we have outlined in this review and elsewhere. It is simpler to hypothesize that the sandpile and multiloops models capture key aspects of the underlying physics, especially those governing global and strongly nonlinear behaviour. The wide range of plasma contexts in which these models succeed furthermore suggests that this physics may be generic to the plasma state.

Imagine that, since the mid-1940s, human existence had faced a serious threat from encroaching sand dunes. In such a situation, the imperative to master sandpile physics would have led, by the 1950s, to a situation where the sandpile model results outlined in this review were already common knowledge. Later, when tokamaks were built, early experimental indications of nonlocality and nondiffusivity in plasma transport, conditioned by critical gradients, would have triggered an avalanche of speculative publications seeking to predict global tokamak phenomenology by analogy with known sandpile model results. The right-hand sides of figures 4 and 5, for example, would have been published as soon as off-axis ECH was considered, and the later arrival of the left-hand sides would then have come as a fulfilment of prediction. The strength of the observational parallels is such that similar hypothetical narratives could be constructed for the magnetospheric and solar coronal examples considered here. The fact that this exercise reverses the historical time sequence is, in some respects, immaterial. While complex systems paradigms did not have the opportunity to produce a predictive *tour de force*, the underlying physical unity remains striking. The degree of agreement between model and observation in figure 5, for example, is about as good as one can get in global nonlinear plasma physics. It leaves little scope for an even better fit, implying that the physics omitted from this intentionally primitive model may not be particularly important. No analogues to figures 5, 7 or 9, for example, have yet been constructed starting from the fundamental equations of plasma physics.

We have shown that the sandpile paradigm, together with related complex systems approaches such as the multiple loops model, can be used to generate good qualitative analogues of many of the distinctive observed elements of global plasma confinement, energy transport and energy release. The complex systems approach is particularly successful in capturing strongly nonlinear phenomena and in generating event statistics for comparison with observed distributions. It can address the emergent physical properties of systems that have very many interacting components acting on a wide range of lengthscales and timescales, which are for this reason inaccessible to conventional *ab initio* approaches. Insofar as complex systems models are successful in these respects, they imply that the dominant elements of the relevant plasma physics may be few and simple. Complex systems models assist identification of these key elements and hold out the prospect of thereby achieving greater practical control and predictive power.

Quantitative progress is taking place in parallel. As noted in section 1, this requires the application to plasmas of modern complex systems methods for characterizing strongly nonlinear or intermittent phenomena. Extreme event statistics, mutual information content, and the differencing and rescaling of turbulence spectra, for example, have been shown (see [4–11] and references therein) to yield quantitative measures that capture key features of the nonlinear behaviour of fusion, space and solar plasmas. The numbers that emerge provide a rigorous, model-independent benchmark for comparison of theory with observation.

Acknowledgments

References

[1] Bak P 1996 *How Nature Works* (New York: Copernicus)
[2] Badii R and Politi A 1999 *Complexity* (Cambridge: Cambridge University Press)
[3] Sornette D 2000 *Critical Phenomena in Natural Sciences* (Heidelberg: Springer)
[4] Dendy R O and Chapman S C 2006 *Plasma Phys. Control. Fusion* **48** B313–28
[5] Greenhough J, Chapman S C, Chaty S, Dendy R O and Rowlands G 2002 *Astron. Astrophys.* **385** 693
[6] Greenhough J, Chapman S C, Chaty S, Dendy R O and Rowlands G 2003 *Mon. Not. R. Astron. Soc.* **340** 851
[7] Greenhough J, Chapman S C, Dendy R O, Nakariakov V and Rowlands G 2003 *Astron. Astrophys.* **409** L17
[8] March T K, Chapman S C and Dendy R O 2005 *Physica* D **200** 171
[9] March T K, Chapman S C and Dendy R O 2005 *Geophys. Res. Lett.* **32** L04101
[10] Dudson B D, Dendy R O, Kirk A, Meyer H and Counsell G C 2005 *Plasma Phys. Control. Fusion* **47** 885
[11] Greenhough J, Chapman S C, Dendy R O and Ward D J 2003 *Plasma Phys. Control. Fusion* **45** 747
[12] Bak P, Tang C and Wiesenfeld K 1987 *Phys. Rev. Lett.* **59** 381
[13] Newman D E, Carreras B A, Diamond P H and Hahm T S 1996 *Phys. Plasmas* **3** 1858
[14] Dendy R O and Helander P 1997 *Plasma Phys. Control. Fusion* **39** 1947
[15] Dendy R O and Helander P 1998 *Phys. Rev.* E **57** 3641
[16] Chapman S C 2000 *Phys. Rev.* E **62** 1905
[17] Sanchez R, Newman D E and Carreras B A 2001 *Nucl. Fusion* **41** 247
[18] Chapman S C, Dendy R O and Hnat B 2001 *Phys. Rev. Lett.* **86** 2814
[19] Graves J P, Dendy R O, Hopcraft K I and Jakeman E 2002 *Phys. Plasmas* **9** 1596
[20] Rhodes T L, Moyer R A, Groebner R, Doyle E J, Peebles W A and Rettig C L 1999 *Phys. Lett.* A **253** 181
[21] Politzer P A 2000 *Phys. Rev. Lett.* **84** 1192
[22] Carreras B A *et al* 1996 *Phys. Plasmas* **3** 2664
[23] Callen J D and Kissick M W 1997 *Plasma Phys. Control. Fusion* **39** B173
[24] Carreras B A *et al* 1998 *Phys. Rev. Lett.* **80** 4438
[25] Pedrosa M A *et al* 1999 *Phys. Rev. Lett.* **82** 3621
[26] Zaslavsky G M *et al* 2000 *Phys. Plasmas* **7** 3691
[27] van Milligen B P, Carreras B A and Sanchez R 2005 *Plasma Phys. Control. Fusion* **47** B743
[28] Garbet X and Waltz R 1998 *Phys. Plasmas* **5** 2836
[29] Sarazin Y and Ghendrih P 1998 *Phys. Plasmas* **5** 4214
[30] Beyer P, Sarazin Y, Garbet X, Ghendrih P and Benkadda S 1999 *Plasma Phys. Control. Fusion* **41** A757
[31] Li J and Kishimoto Y 2002 *Phys. Rev. Lett.* **89** 115002
[32] Tangri V, Das A, Kaw P and Singh R 2003 *Phys. Rev. Lett.* **91** 025001
[33] Villard L *et al* 2004 *Plasma Phys. Control. Fusion* **46** B51
[34] Chapman S C, Dendy R O and Rowlands G 1999 *Phys. Plasmas* **6** 4169

[35] Chapman S C, Dendy R O and Hnat B 2003 *Plasma Phys. Control. Fusion* **45** 301

[36] March T K, Chapman S C, Dendy R O and Merrifield J A 2004 *Phys. Plasmas* **11** 659

[37] Fishpool G M 1998 *Nucl. Fusion* **38** 1373

[38] Luce T C, Petty C C and de Haas J C M 1992 *Phys. Rev. Lett.* **68** 52

[39] Petty C C and Luce T C 1994 *Nucl. Fusion* **34** 121

[40] de Baar M R, Hogeweij G M D, Lopes Cardozo N J, Oomens A A M and Schüller F C 1997 *Phys. Rev. Lett.*
       78 4573

[41] de Baar M R *et al* 1999 *Phys. Plasmas* **6** 4645

[42] Chapman S C, Dendy R O and Watkins N W 2004 *Plasma Phys. Control. Fusion* **46** B157

[43] Tsurutani B *et al* 1990 *Geophys. Res. Lett.* **17** 279

[44] Takalo J and Timonen J 1998 *Geophys. Res. Lett.* **25** 2101

[45] Consolini G 1997 *Cosmic Physics in the Year 2000* (Bologna, Italy: Società Italiana di Fisica) p 123

[46] Chapman S C, Watkins N W, Dendy R O, Helander P and Rowlands G 1998 *Geophys. Res. Lett.* **25** 2397

[47] Watkins N W, Freeman M P, Chapman, S C and Dendy R O 2001 *J. Atmos. Sol.-Terr. Phys.* **63** 1435

[48] Chapman S C, Dendy R O and Hnat B 2001 *Phys. Plasmas* **8** 1969

[49] Hnat B, Chapman S C, Rowlands G, Watkins N W and Freeman M P 2003 *Geophys. Res. Lett.* **30** 2174

[50] Watkins N W, Chapman S C, Dendy R O, Helander P and Rowlands G 1999 *Geophys. Res. Lett.* **26** 2617

[51] Lui A T Y, Chapman S C, Liou K, Newell P T, Meng C I, Brittnacher M and Parks G K 2000 *Geophys. Res.*
       Lett. **27** 911

[52] Parker E N 1983 *Astrophys. J.* **264** 642
       Parker E N 1988 *Astrophys. J.* **330** 474
       Parker E N 1994 *Spontaneous Current Sheets in Magnetic Fields* (New York: Oxford University Press)

[53] Priest E R and Forbes T 2000 *Magnetic Reconnection* (Cambridge: Cambridge University Press)

[54] Hughes D, Paczuski M, Dendy R O, Helander P and McClements K 2003 *Phys. Rev. Lett.* **90** 131101

[55] Schrijver C J *et al* 1998 *Nature* **394** 152; see also http://www.lmsal.com/carpet.htm

[56] Dennis B R 1985 *Sol. Phys.* **100** 465

[57] Aschwanden M J *et al* 2000 *Astrophys. J.* **535** 1047

[58] Wheatland M J, Sturrock P A and McTiernan J M 1998 *Astrophys. J.* **509** 448

[59] Charbonneau P, McIntosh S W, Liu H-L and Bogdan T J 2001 *Sol. Phys.* **203** 321

[60] Lu E T and Hamilton R J 1991 *Astrophys. J.* **380** L89

[61] Turcotte D L 1999 *Rep. Prog. Phys.* **62** 1377